HAL
open science

Non standard thermodynamics framework for robust computations with induced anisotropic damage

Rodrigue Desmorat, Fabrice Gatuingt, Frédéric Ragueneau

To cite this version:

Rodrigue Desmorat, Fabrice Gatuingt, Frédéric Ragueneau. Non standard thermodynamics framework for robust computations with induced anisotropic damage. International Journal of Damage Mechanics, 2010, 19 (1), pp.53-73. 10.1177/1056789509104839 . hal-00994281

HAL Id: hal-00994281

https://hal.science/hal-00994281

Submitted on 21 May 2014

HAL is a multi-disciplinary open access archive for the deposit and dissemination of scientific research documents, whether they are published or not. The documents may come from teaching and research institutions in France or abroad, or from public or private research centers.

L'archive ouverte pluridisciplinaire **HAL**, est destinée au dépôt et à la diffusion de documents scientifiques de niveau recherche, publiés ou non, émanant des établissements d'enseignement et de recherche français ou étrangers, des laboratoires publics ou privés.

Non standard thermodynamics framework for robust computations with induced anisotropic damage

R. Desmorat, F. Gatuingt & F. Ragueneau
LMT-Cachan
ENS Cachan / Univ. Paris 6 / CNRS / UniverSud Paris
61 av. du président Wilson
F-94235 Cachan Cedex, France

Abstract

ABSTRACT: Many anisotropic damage models have been proposed for different materials, including concrete. The main drawback of the corresponding analyses is that a large number of material parameters is often introduced, leading to identification difficulties but also to model complexity and associated numerical difficulties. It is also sometimes difficult to ensure the continuity of the stresses if the quasi-unilateral effect of microcracks closure and the dissymmetry tension/compression are represented.

In order to solve those difficulties, one proposes to write the damage models in a specific non standard thermodynamics framework. The damage states are represented by a symmetric second order tensor and the damage rate is assumed governed by a positive second order tensor having a clear meanning: the absolute or the positive value of the plastic strain rate tensor for ductile materials, the positive part of the total strain tensor in quasi-brittle materials. Such a non standard feature makes the proof of the the positivity of the intrinsic dissipation necessary. This important proof is given in the considered framework for any damage law ensuring (anisotropic) damage increase and for any case, 3D, proportional or non proportional. This extends then to induced anisotropy the isotropic case property of a positive damage rate as a sufficient condition for the thermodynamics second principle to be fulfilled.

Altogether with the fact that the thermodynamics potential can be continuously differentiated, the anisotropic damage model for concrete (build in this framework) allows for robust Finite Element implementation. Both space (classical nonlocal with internal length, nonlocal with internal time) and time regularizations (visco- or delay-damage) are used and applied to quasi-static and dynamic cases. Examples on concrete and reinforced concrete structures are given.

1 INTRODUCTION

In standard thermodynamics framework (Halphen and Nguyen, 1975) both the state and the evolution laws derive from potentials, Gibbs free enthalpy

$\rho\psi^\star$ written in terms of stress $\boldsymbol{\sigma}$ in the present work for the first one, a dissipation or pseudo-dissipation potential for the second one. The elasticity law and the strain energy release rate density $\boldsymbol{Y}$, variable associated with $\boldsymbol{D}$, are respectively gained as the derivative of the state potential with respect to the elastic strain tensor $\boldsymbol{\epsilon}^e$ and with respect to the damage tensor $\boldsymbol{D}$. In the standard framework of thermodynamics a pseudo-dissipation potential quadratic function of $\boldsymbol{Y}$ is most often considered, the damage law taking the form

$$\dot{\boldsymbol{D}} = \dot{\lambda}\, \underline{\boldsymbol{J}} : \boldsymbol{Y} \tag{1}$$

with $\dot{\lambda}$ a positive multiplier and $\underline{\boldsymbol{J}}$ a positive fourth order tensor, eventually nonlinear function of the thermodynamics variables, so that the dissipation

$$\mathcal{D} = \boldsymbol{Y} : \dot{\boldsymbol{D}} = \dot{\lambda}\, \boldsymbol{Y} : \underline{\boldsymbol{J}} : \boldsymbol{Y} \tag{2}$$

due to the degradation mechanisms remains positive for any kind of loading. The choice of damage laws of the form (1) is very restrictive, for instance concerning the possibility to model induced anisotropy directly driven by the strains or the stresses. But, as we will illustrate on numerical examples, to ensure the positivity of the intrinsic dissipation also has good numerical properties.

2 NON STANDARD ANISOTROPIC FRAMEWORK

2.1 *State potential*

A general form for the strain energy coupled with anisotropic damage has been proposed by Ladevèze (Ladevèze, 1983; Lemaitre and Desmorat, 2005), as

$$\rho\psi^\star = a_1\, tr\,(\boldsymbol{H\sigma H\sigma}) + a_2\, \boldsymbol{\sigma} : \boldsymbol{\sigma} + a_3\, g(D_H)(tr\, \boldsymbol{\sigma})^2 + a_4\, (tr\, \boldsymbol{\sigma})^2 \tag{3}$$

with

$$\boldsymbol{H} = (\boldsymbol{1} - \boldsymbol{D})^{-1/2} \tag{4}$$

a symmetric tensor and

$$D_H = \frac{1}{3} tr\, \boldsymbol{D} \tag{5}$$

$g(D_H)$ is a positive increasing function of D_H, for example $g(D_H) = 1/(1 - \eta D_H)$. The a_i ($a_1 \geq 0$, $a_3 \geq 0$) as well as $\eta > 0$ are material parameters. The first term of Eq. (3) can take different – non equivalent – forms (Ladevèze, 1983; Ladevèze, 1995; Papa and Taliercio, 1996; Lemaitre and Desmorat, 2005),

$$a_1\, tr\left(\boldsymbol{H\sigma}^D \boldsymbol{H\sigma}^D\right) \tag{6}$$

where $(.)^D$ denotes the deviatoric part, or

$$a_1 \left[\, tr\,(\boldsymbol{H\sigma}_+ \boldsymbol{H\sigma}_+) + \langle \boldsymbol{\sigma} \rangle_- : \langle \boldsymbol{\sigma} \rangle_- \right] \tag{7}$$

or

$$a_1 \left[\, tr\left(\boldsymbol{H\sigma}_+^D \boldsymbol{H\sigma}_+^D\right) + \left\langle \boldsymbol{\sigma}^D \right\rangle_- : \left\langle \boldsymbol{\sigma}^D \right\rangle_- \right] \tag{8}$$

allowing in the last case for the mechanical representation of the quasi-unilateral effect of micro-defects closure, with $\boldsymbol{\sigma}_+$ (resp. $\boldsymbol{\sigma}_+^D$) a special

positive part (Ladevèze, 1983; Desmorat, 2000; Desmorat and Cantournet, 2008) built from the eigenvalues and the eigenvectors of $\boldsymbol{H\sigma}$ (resp. of $\boldsymbol{H\sigma}^D$) and with $\langle . \rangle_-$ the negative part in terms of principal components of a tensor. Two examples of strain energy densities are a first one based on a splitting deviatoric / hydrostatic quantities (with E and ν the Young's modulus and Poisson's ratio of the undamaged material and η a shear-bulk coupling parameter (Lemaitre et al., 2000; Delaplace and Desmorat, 2007)),

$$\rho\psi^\star = \frac{1+\nu}{2E} tr\left(\boldsymbol{H\sigma}^D \boldsymbol{H\sigma}^D\right) + \frac{1-2\nu}{6E}\frac{(tr\,\boldsymbol{\sigma})^2}{1-\eta D_H} \tag{9}$$

a second one based on the feature of a constant ν/E ratio,

$$\rho\psi^\star = \frac{1}{2E}\, tr\left(\boldsymbol{H\sigma H\sigma}\right) + \frac{\nu}{2E}\left(\,\boldsymbol{\sigma}:\boldsymbol{\sigma} - (tr\,\boldsymbol{\sigma})^2\right) \tag{10}$$

2.2 *Non standard damage evolution laws*

Concerning the evolution laws, many non standard damage laws can be formulated for induced anisotropy (Mazars et al., 1990; Dragon and Halm, 1996; Lemaitre et al., 2000; Billardon and Pétry, 2005), with second order tensorial damage rate proportional

- to the positive part of the strain tensor $\langle \boldsymbol{\epsilon} \rangle_+$ or to $\langle \boldsymbol{\epsilon} \rangle_+^\alpha$ with α a damage exponent,
- to the absolute value of the plastic strain tensor $\dot{\boldsymbol{\epsilon}}^p$, to the positive part of $\dot{\boldsymbol{\epsilon}}^p$, or to any linear combination $\zeta\,|\dot{\boldsymbol{\epsilon}}^p| + (1-\zeta)\,\langle \dot{\boldsymbol{\epsilon}}^p \rangle_+$,
- to a power $2s$ of the stress tensor,
- to a linear combination $\zeta\,\langle \boldsymbol{\sigma} \rangle_+^2 + (1-\zeta)\,\langle \boldsymbol{\sigma} \rangle_-^2$ (eventually at the power s) where to take $\zeta = 1$ will lead to the modeling of the unilateral damage effect of no damage growth in compression, and to take $1/2 < \zeta < 1$ will lead to the modeling of the quasi-unilateral damage effect of a damage growth in compression smaller than in tension.

Induced damage anisotropy governed by the positive extensions is adapted to quasi-brittle materials as concrete. The other expressions will allow to generalize to induced anisotropy Lemaitre's damage law

$$\dot{D} = \left(\frac{Y}{S}\right)^s \dot{p} \tag{11}$$

of a damage rate governed by the accumulated plastic strain rate $\dot{p}$ and enhanced by the strain energy

$$Y = \frac{1}{2}\boldsymbol{\epsilon}^e : \underline{\boldsymbol{E}} : \boldsymbol{\epsilon}^e \tag{12}$$

with $\underline{\boldsymbol{E}}$ Hooke's tensor. As possible generalization, one has

$$\dot{\boldsymbol{D}} = \left(\frac{Y}{S}\right)^s \left[\zeta\,|\dot{\boldsymbol{\epsilon}}^p| + (1-\zeta)\,\langle \dot{\boldsymbol{\epsilon}}^p \rangle_+\right] \tag{13}$$

$$\dot{\boldsymbol{D}} = \left(\frac{\zeta\,\langle \boldsymbol{\sigma} \rangle_+^2 + (1-\zeta)\,\langle \boldsymbol{\sigma} \rangle_-^2}{2ES}\right)^s \dot{p} \tag{14}$$

where E denotes the Young's modulus and S and s the damage parameters. For more details on ductile damage, refer to (Lemaitre and Desmorat, 2005).

The next question will be wether one automatically can ensure the positvity of the dissipation with the simple feature of a positive (tensorial) damage rate $\dot{\boldsymbol{D}}$.

2.3 *Link with fourth order damage*

The elasticity law corresponding to Gibbs potential (3) is

$$\boldsymbol{\epsilon}^e = \rho \frac{\partial \psi^\star}{\partial \boldsymbol{\sigma}} = 2a_1\, \boldsymbol{H}\boldsymbol{\sigma}\boldsymbol{H} + 2a_2\, \boldsymbol{\sigma} + 2\left(a_3\, g(D_H) + a_4\right)\, tr\, \boldsymbol{\sigma}\, \mathbf{1} \tag{15}$$

It can used to exhibit the fourth order effective elasticity tensor as $\boldsymbol{\epsilon}^e = \underline{\tilde{\boldsymbol{E}}}^{-1} : \boldsymbol{\sigma}$ and then

$$\underline{\tilde{\boldsymbol{E}}}^{-1}(\boldsymbol{D}) = 2a_1\, \boldsymbol{H}\underline{\overline{\otimes}}\boldsymbol{H} + 2a_2\, \underline{\boldsymbol{I}} + 2\left(a_3\, g(D_H) + a_4\right)\, \mathbf{1} \otimes \mathbf{1} \tag{16}$$

with $\mathbf{1}$ and $\boldsymbol{I}$ respectively the second and fourth order unit tensors and where $(\boldsymbol{H}\underline{\overline{\otimes}}\boldsymbol{H})_{ijkl} = \frac{1}{2}(H_{ik}H_{jl} + H_{il}H_{jk})$ and with

$$a_1 + a_2 = \frac{1+\nu}{2E} \qquad a_3\, g(0) + a_4 = -\frac{\nu}{2E} \tag{17}$$

Different expressions corresponds to different choices of material parameters a_i. Micromechanics and homogeneization calculations a of medium with cracks and cavities can be used as guidelines for such choices. A fourth order damage tensor $\underline{\boldsymbol{D}}$ can then be built from $(\underline{\boldsymbol{I}} - \underline{\boldsymbol{D}}) : \underline{\boldsymbol{E}} = \underline{\tilde{\boldsymbol{E}}}$ as

$$\underline{\boldsymbol{D}} = \underline{\boldsymbol{I}} - \underline{\boldsymbol{E}}^{-1} : \underline{\tilde{\boldsymbol{E}}} \tag{18}$$

The *a priori* choice of a state potential is a limitation of the modelling, as one knows that the second order damage representation is only an approximation (Leckie and Onat, 1981; Krajcinovic, 1996): systematic studies in non proportional loading cases are needed to fully validate any damage model built in present non standard framework (this applies to the damage model for concrete considered next).

But note that the direct use of fourth order damage in phenomenological constitutive models often leads to a damage anisotropy difficult to visualize (6 principal damages instead of 3 for the second order framework) and to too many damage parameters.

3 POSITIVITY OF THE INTRINSIC DISSIPATION

Previous elastic energy densities can be continuously differentiated as

$$d\rho\psi^\star = \boldsymbol{\epsilon}^e : d\boldsymbol{\sigma} + \boldsymbol{Y} : d\boldsymbol{D} \tag{19}$$

or

$$\begin{aligned} d\rho\psi^\star = {} & [2a_1\left(\boldsymbol{H}\boldsymbol{\sigma}\boldsymbol{H}\right) + 2a_2\, \boldsymbol{\sigma} + 2a_3\, g(D_H)\, tr\, \boldsymbol{\sigma}\, \mathbf{1} + 2a_4\, tr\, \boldsymbol{\sigma}\, \mathbf{1}] : d\boldsymbol{\sigma} \\ & + 2a_1\left(\boldsymbol{\sigma}\boldsymbol{H}\boldsymbol{\sigma}\right) : d\boldsymbol{H} + \frac{1}{3} a_3\, g'(D_H)(tr\, \boldsymbol{\sigma})^2\, tr\, d\boldsymbol{D} \end{aligned} \tag{20}$$

leading to a dissipation due to damage mechanisms expressed as

$$\mathcal{D} = \boldsymbol{Y} : \dot{\boldsymbol{D}} = 2a_1\,(\boldsymbol{\sigma H \sigma}) : \dot{\boldsymbol{H}} + \frac{1}{3} a_3\, g'(D_H)(tr\,\boldsymbol{\sigma})^2\; tr\,\dot{\boldsymbol{D}} \tag{21}$$

For the elastic energy densities written with the terms (6) or (8), the first term $2a_1\,(\boldsymbol{\sigma H \sigma}) : \dot{\boldsymbol{H}}$ must be replaced by $2a_1\left(\boldsymbol{\sigma}^D \boldsymbol{H} \boldsymbol{\sigma}^D\right) : \dot{\boldsymbol{H}}$ or $2a_1\,(\boldsymbol{\sigma}_+ \boldsymbol{H} \boldsymbol{\sigma}_+) : \dot{\boldsymbol{H}}$ or $2a_1\left(\boldsymbol{\sigma}_+^D \boldsymbol{H} \boldsymbol{\sigma}_+^D\right) : \dot{\boldsymbol{H}}$. These terms are next synthetically written

$$2a_1\,(\boldsymbol{s H s}) : \dot{\boldsymbol{H}} \tag{22}$$

With any damage law leading to a positive damage rate tensor, i.e. with positives eigenvalues $(\dot{\boldsymbol{D}})_J$, the term

$$tr\,\dot{\boldsymbol{D}} = \sum_{J=1}^{3} (\dot{\boldsymbol{D}})_J \tag{23}$$

is positive so that

$$\frac{1}{3} a_3\, g'(D_H)(tr\,\boldsymbol{\sigma})^2\; tr\,\dot{\boldsymbol{D}} \geq 0 \tag{24}$$

It is important to precise that the eigenvalues $(\dot{\boldsymbol{D}})_J$ of $\dot{\boldsymbol{D}}$ are not the derivatives $\dot{D}_J$ of the eigenvalues of $\boldsymbol{D}$ (except in the particular case where $\boldsymbol{D}$ and $\dot{\boldsymbol{D}}$ have the same principal directions), the positivity of the eigenvalues $(\dot{\boldsymbol{D}})_J$ nevertheless implies the increase of the eigenvalues of $\boldsymbol{D}$.

Concerning the term $2a_1(\boldsymbol{s H s}) : \dot{\boldsymbol{H}}$, note that the expression $\boldsymbol{H} = (\boldsymbol{1} - \boldsymbol{D})^{-1/2}$ rewritten in terms of principal components

$$H_J = \frac{1}{\sqrt{1 - D_J}} \tag{25}$$

gives positive increasing eigenvalues H_J of tensor $\boldsymbol{H}$ which is then also positive and increasing during any damage process. The positivity of the symmetric matrix $(\boldsymbol{s H s})$ is gained by seeking the sign of its eigenvalues, denoted χ, solution of

$$(\boldsymbol{s H s})\,\vec{g} = \chi\,\vec{g} \tag{26}$$

with $\vec{g}$ the corresponding eigenvectors. The eigenvalues χ are equivalently solution of

$$(\boldsymbol{H s})^2 \vec{g} = \chi\,\boldsymbol{H}\vec{g} \tag{27}$$

with obviously $(\boldsymbol{H s})^2$ a positive matrix. These eigenvalues take the form

$$\chi = \frac{\vec{g}^T (\boldsymbol{H s})^2 \vec{g}}{\vec{g}^T \boldsymbol{H} \vec{g}} \tag{28}$$

and, as ratio of positive terms, are positive.

Last, the tensorial product $(\boldsymbol{s H s}) : \dot{\boldsymbol{H}}$ of two symmetric positive tensors $(\boldsymbol{s H s})$ and $\dot{\boldsymbol{H}}$ being positive, one can conclude to the positivity of the intrinsic dissipation $\mathcal{D}$ for any damaging loading, monotonic or not, uniaxial or multiaxial, proportional or non proportional... at the simple condition extended here to anisotropic damage that the damage rate $\dot{\boldsymbol{D}}$ must remain a positive tensor.

Considering conversely the set of states represented by deviatoric tensors $\boldsymbol{\sigma} = \boldsymbol{\sigma}^D$, the dissipation reduced to $2a_1\,(\boldsymbol{s H s}) : \dot{\boldsymbol{H}} \geq 0 \quad \forall\,(\boldsymbol{s H s}) \geq \boldsymbol{0}$ leads to $\dot{\boldsymbol{H}} \geq \boldsymbol{0}$, therefore to the fact that $\dot{\boldsymbol{D}} \geq \boldsymbol{0}$ is a necessary and sufficient condition for the positivity of the dissipation due to damage $\mathcal{D} = \boldsymbol{Y} : \dot{\boldsymbol{D}}$.

4 ANISOTROPIC DAMAGE MODEL FOR CONCRETE

An anisotropic damage model has been proposed for concrete in previous non standard thermodynamics framework (Desmorat, 2004; Desmorat et al., 2007) introducing a single damage variable, a second order tensor, as the representation of the damage state due to microcracking. Mainly due to induced anisotropy, the dissymmetric response of concrete in tension and in compression is obtained with a low number of material parameters (figure 1): 2 for elasticity, 1 as damage threshold, 2 for damage evolution. Mazars strain damage criterion (Mazars, 1984) is used in this initial model, with the advantage of simplicity for instance at the numerical level.

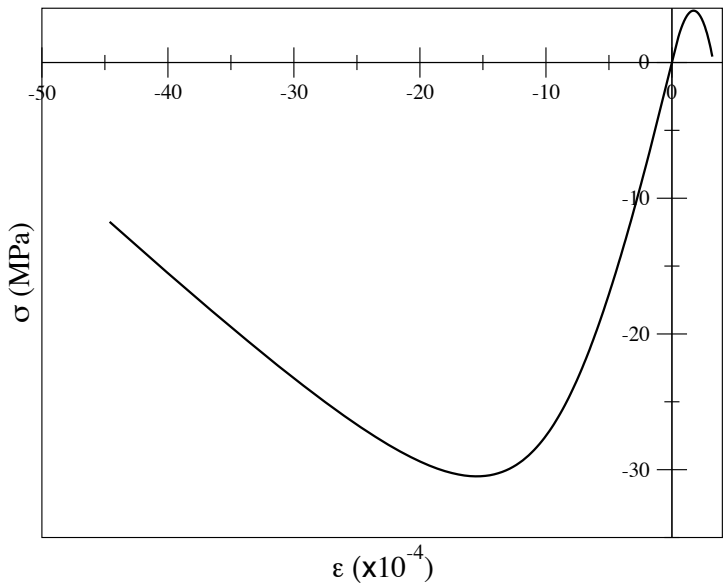

Figure 1: Response of the model in tension and compression ($E = 37$ GPa, $\nu = 0.2$, $\kappa_0 = 5 \cdot 10^{-5}$, $a = 3 \cdot 10^{-4}$, $A = 5 \cdot 10^3$).

4.1 *Induced anisotropic damage model*

For concrete, the microcracks due to tension are mainly orthogonal to the loading direction, when the microcracks due to compression are mainly parallel to the loading direction. The damage state has then to be represented by a tensorial variable $\boldsymbol{D}$ either a fourth rank tensor or a second rank tensor. The use of a second order damage tensor is more convenient for practical applications (as well as for the material parameters identification) and this is the choice made here. The damage anisotropy induced by either tension or compression is simply modeled by the consideration of damage evolution laws ensuring a damage rate proportional to the positive part of the strain tensor, i.e. a damage governed by the principal extensions (Mazars et al., 1990).

The full set of constitutive equations reads:

- Elasticity,

$$\boldsymbol{\epsilon} = \frac{1+\nu}{E}\tilde{\boldsymbol{\sigma}} - \frac{\nu}{E} tr\, \tilde{\boldsymbol{\sigma}}\, \mathbf{1} \quad \text{or} \quad \boldsymbol{\epsilon} = \underline{\boldsymbol{E}}^{-1} : \tilde{\boldsymbol{\sigma}} \tag{29}$$

- Effective stress ($(.)^D$ standing for the deviatoric part),

$$\begin{aligned} \tilde{\boldsymbol{\sigma}} = & \left[(\mathbf{1} - \boldsymbol{D})^{-1/2}\, \boldsymbol{\sigma}^D\, (\mathbf{1} - \boldsymbol{D})^{-1/2} \right]^D \\ & + \frac{1}{3} \left[\frac{\langle tr\, \boldsymbol{\sigma} \rangle_+}{1 - tr\, \boldsymbol{D}} + \langle tr\, \boldsymbol{\sigma} \rangle_- \right] \mathbf{1} \end{aligned} \tag{30}$$

- Damage criterion $f = \hat{\epsilon} - \kappa(tr\, \boldsymbol{D})$, so that the condition $f < 0 \longrightarrow$ elastic loading or unloading, $f = 0$, $\dot{f} = 0 \longrightarrow$ damage growth, where $\hat{\epsilon} = \sqrt{\langle \boldsymbol{\epsilon} \rangle_+ : \langle \boldsymbol{\epsilon} \rangle_+}$ is Mazars equivalent strain and where

$$\kappa^{-1}(\hat{\epsilon}) = aA \left[\arctan\left(\frac{\hat{\epsilon}}{a}\right) - \arctan\left(\frac{\kappa_0}{a}\right) \right] \tag{31}$$

  introducing κ_0 as damage threshold, A and a as damage parameters.

- Induced damage anisotropy governed by the positive extensions,

$$\dot{\boldsymbol{D}} = \dot{\lambda} \langle \boldsymbol{\epsilon} \rangle_+^2 \tag{32}$$

  The damage multiplier $\dot{\lambda}$ is determined from the consistency condition $f = 0$, $\dot{f} = 0$.

The use of a damage criterion function f written in terms of strains instead of stresses allows for a simple implementation in a Finite Element computer code (Desmorat et al., 2007). Even if Euler backward scheme is used, there is no need of an iterative process. Note that at the final stage of numerical implementation the elasticity law needs to be inverted. This can be done in a closed form as:

$$\begin{aligned} \boldsymbol{\sigma} = & (\mathbf{1} - \boldsymbol{D})^{1/2}\, \tilde{\boldsymbol{\sigma}}\, (\mathbf{1} - \boldsymbol{D})^{1/2} - \frac{(\mathbf{1} - \boldsymbol{D}) : \tilde{\boldsymbol{\sigma}}}{3 - tr\, \boldsymbol{D}} (\mathbf{1} - \boldsymbol{D}) \\ & + \frac{1}{3} \left[(1 - tr\, \boldsymbol{D}) \langle tr\, \tilde{\boldsymbol{\sigma}} \rangle_+ + \langle tr\, \tilde{\boldsymbol{\sigma}} \rangle_- \right] \mathbf{1} \end{aligned} \tag{33}$$

4.2 *Extension to nonlocal*

Classical mesh dependency occurs when using previous local damage model in a Finite Element code. A nonlocal regularization can be used to gain the mesh independency. One just has to replace local Mazars strain $\hat{\epsilon}$ in the damage criterion f by nonlocal Mazars strain $\hat{\epsilon}^{nl}$ and to consider as nonlocal criterion,

$$f = \hat{\epsilon}^{nl} - \kappa \tag{34}$$

where nonlocal equivalent strain can be defined using an integral form with $\mathcal{W}(\xi^2)$ a nonlocal weight function (Pijaudier-Cabot and Bazant, 1987), usually a gaussian function $e^{-4\xi^2}$ or a bell-shaped function $\langle 1 - \xi^2 \rangle_+^2$,

$$\begin{aligned} \hat{\epsilon}^{nl}(\mathbf{x}) &= \frac{1}{V_r} \int_\Omega \mathcal{W}\left(\frac{\|\mathbf{x} - \mathbf{s}\|^2}{\ell_c^2} \right) \hat{\epsilon}(\mathbf{s})\, ds \\ V_r(\mathbf{x}) &= \int_\Omega \mathcal{W}\left(\frac{\|\mathbf{x} - \mathbf{s}\|^2}{\ell_c^2} \right) ds \end{aligned} \tag{35}$$

or using a second gradient form (Aifantis, 1987; Peerlings et al., 1996),

$$\hat{\epsilon}^{nl} - \gamma\, \nabla^2 \hat{\epsilon}^{nl} = \hat{\epsilon} \tag{36}$$

Both the integral form (through $\mathcal{W}$) and the gradient form (through γ) introduce a characteristic length ℓ_c.

Nevertheless, and as pointed out by (Pijaudier-Cabot et al., 2004) from acoustic emission measurements during the damage process, the internal length is evolving with damage and is therfore probably better represented by a positive fourth order tensor $\underline{\boldsymbol{w}}$ function of $\boldsymbol{D}$ instead of the scalar ℓ_c. This can be done formally by replacing

$$\mathcal{W}\left(\frac{\|\mathbf{x}-\mathbf{s}\|^2}{\ell_c^2}\right) \quad \text{by} \quad \mathcal{W}\left((\mathbf{x}-\mathbf{s}) : \underline{\boldsymbol{w}}(\boldsymbol{D}) : (\mathbf{x}-\mathbf{s})\right) \tag{37}$$

in previous integral equations. The isotropic scalar internal length theory is the particular case $\underline{\boldsymbol{w}} = \ell_c^{-2}\underline{\boldsymbol{I}}$. In the same spirit, the gradient term $\gamma\, \nabla^2 \hat{\epsilon}^{nl}$ may be rewritten $\nabla(\boldsymbol{\Gamma}\nabla\hat{\epsilon}^{nl})$ with $\boldsymbol{\Gamma} = \boldsymbol{\Gamma}(\boldsymbol{D})$ an evolving second order tensor.

An other possibility, naturally taking into account the effect of damage (therefore its anisotropy in terms of internal lengths, for second order damage as well as for fourth order damage), is to consider an internal time τ_c instead of ℓ_c and to replace the argument of the weight function $\mathcal{W}$ by the ratio τ_{xs}/τ_c, i.e.

$$\mathcal{W}\left(\frac{\|\mathbf{x}-\mathbf{s}\|^2}{\ell_c^2}\right) \quad \text{replaced by} \quad \mathcal{W}\left(\frac{\tau_{xs}}{\tau_c}\right) \tag{38}$$

The time τ_{xs} is the time for the deformation information to go from point $\mathbf{s}$ to point $\mathbf{x}$ (calculated by wave propagation, wave speed affected by damage denoted $\tilde{c}$). When $\boldsymbol{D} = 0$ this formulation is equivalent to Pijaudier-Cabot and Bazant nonlocal theory: then $\tau_{xs} = \|\mathbf{x}-\mathbf{s}\|/c$ and $\tau_c = \ell_c/c = Cst$ is set ($c = \tilde{c}(\boldsymbol{D} = 0)$ is the wave speed of the virgin material).

To take into account in finite elements computations an evolving internal length means to actualize at each time step and for each couple $(\mathbf{x}, \mathbf{s})$ the value of the weight function. This (very) costly choice is not made here. Even if induced anisotropy is considered next, the introduction of a single (constant) internal length will be considered as sufficient for practical applications.

5 VISCOUS REGULARIZATION FOR IMPACT

A regularization possibility for fast dynamics and impact consists in taking into account the strain rate effect on the dynamic response of concrete. For instance, introduce a characteristic time which, altogether with the consideration of the laws of dynamics, will indirectly defines a characteristic length. In the present case of elasticity coupled with damage this can simply be done by introducing a viscosity law $\epsilon_v = \epsilon_v(\dot{D})$ in Mazars criterion. The damage evolution occurs not anymore at $f = 0$ but at $f = \epsilon_v > 0$. A classical law for isotropic damage is Norton-Perzyna power law, $\epsilon_v = k\dot{D}^{1/n}$, with k and n the viscosity parameters. It leads to an unbounded damage rate often too high at high strain rates.

It is possible to bound the damage rate, for instance by the maximum rate $\dot{D}_\infty = 1/\tau_c$ material dependent equal to the inverse of the characteristic time τ_c (Allix and Deü, 1997; Ladevèze et al., 1998). To gain this property, these authors rewrite the criterion surface as $f = g(\hat{\epsilon}) - D$ (with $g = \kappa^{-1}$) and define the viscosity law as

$$f = D_v > 0 \qquad D_v = -\frac{1}{b}\ln\left(\frac{\dot{D}_\infty - \dot{D}}{\dot{D}_\infty}\right) \tag{39}$$

from which derives the delay-damage law, saturating at high strain rates,

$$\dot{D} = \dot{D}_\infty\left[1 - \exp\left(-b(g(\hat{\epsilon}) - D)\right)\right] \tag{40}$$

The viscosity parameters, material dependent, are then $\dot{D}_\infty$ and b. This regularization is defined locally (i.e. at a structure Gauss point) and is well adapted for dynamics computations. It can be extended to the case of induced anisotropic damage by setting (Desmorat et al., 2008):

$$tr\,\dot{\boldsymbol{D}} = \dot{D}_\infty\left[1 - \exp\left(-b\left(\kappa^{-1}(\hat{\epsilon}) - tr\,\boldsymbol{D}\right)\right)\right] \tag{41}$$

The full set of constitutive equations now reads:

- Elasticity,

$$\boldsymbol{\epsilon} = \frac{1+\nu}{E}\tilde{\boldsymbol{\sigma}} - \frac{\nu}{E}tr\,\tilde{\boldsymbol{\sigma}}\,\mathbf{1} \quad \text{or} \quad \boldsymbol{\epsilon} = \underline{\boldsymbol{E}}^{-1} : \tilde{\boldsymbol{\sigma}} \tag{42}$$

- Effective stress,

$$\begin{aligned}\tilde{\boldsymbol{\sigma}} = &\left[(\mathbf{1} - \boldsymbol{D})^{-1/2}\,\boldsymbol{\sigma}^D\,(\mathbf{1} - \boldsymbol{D})^{-1/2}\right]^D \\ &+ \frac{1}{3}\left[\frac{\langle tr\,\boldsymbol{\sigma}\rangle_+}{1 - tr\,\boldsymbol{D}} + \langle tr\,\boldsymbol{\sigma}\rangle_-\right]\mathbf{1}\end{aligned} \tag{43}$$

- Damage criterion (local) $f = \kappa^{-1}(\hat{\epsilon}) - tr\,\boldsymbol{D}$, using the viscous regularization (39),

$$\begin{aligned}&f \leq 0 \longrightarrow \text{elastic loading or unloading} \\ &f > 0 \;\text{ with }\; f = -\frac{1}{b}\ln\left(\frac{\dot{D}_\infty - tr\,\dot{\boldsymbol{D}}}{\dot{D}_\infty}\right) \\ &\qquad\longrightarrow \text{damage growth}\end{aligned} \tag{44}$$

  with $\dot{D}_\infty$ and b the delay-damage parameters.

- Induced damage anisotropy governed by the positive extensions,

$$\dot{\boldsymbol{D}} = \dot{\lambda}\langle\boldsymbol{\epsilon}\rangle_+^2 \tag{45}$$

  The damage multiplier $\dot{\lambda}$ is determined from the damage criterion expression for $f > 0$ (Eq. 44).

The delay-damage law (40) is recovered from previous equations.

Again, the numerical implementation in a Finite Elements computer code is quite simple as – once again – it does not need an iterative process (Desmorat et al., 2008).

6 STRUCTURAL EXAMPLES

The local and nonlocal integral anisotropic damage model has been implemented in CEA CAST3M Finite Element code. The anisotropic delay-damage model has been implemented in the explicit code LS-Dyna. The numerical scheme for the time integration is for both cases Euler's backward scheme but solved explicitly (Desmorat et al., 2007; Desmorat et al., 2008). Finite Element examples on 3D structures are given next to illustrate the model capabilities.

6.1 *Plain concrete mixed-mode fracture*

The double edge notched specimen tested by Nooru-Mohamed (Nooru-Mohamed, 1992) is analysed using the implementation of the model developed in the previous section. The specimen is a symmetric 200 mm$\times$ 200 mm mortar square with two horizontal notches, 30 mm long and 5 mm thick.

The rotation of the external boundary of the plate is restricted around the vertical axis. The concrete specimen is first loaded by an increasing shear (lateral) force $F(t)$ applied on the lateral surface. During the application of the shear force, the vertical displacement of the upper surface is totally free. In a second time, a vertical displacement $U(t)$ is applied up to failure at constant $F = F_{Max}$, the higher F_{Max} the more curved the crack path.

The case study is here carried out for a lateral load $F_{Max} = 10$ kN. The FE discretization of the specimen is made by the use of four node tetrahedron elements with one integration point. In order to perform the computations in 3D at reasonable cost, a FE mesh with a 5 mm width is used when the real width of the specimen is 50 mm. The model parameters used for the simulation are: $E = 42000$ MPa, $\nu = 0.2$, $\kappa_0 = 5\ 10^{-5}$, $A = 5\ 10^3$, $a = 2.93\ 10^{-4}$. The nonlocal length used in the integral weight function is $\ell_c = 2$ mm, small value indeed justified by the fact that the material is a mortar with very small constituents (Bazant and Pijaudier-Cabot, 1989; Ragueneau et al., 2003). Three meshes are used: a coarse mesh with a total of 4936 elements, a medium mesh with 11294 elements, and a fine mesh with 14766 elements. The characteristic length corresponds then close to the notch to 2 elements of the coarse mesh, to 8 elements of the medium mesh, to 14 elements of the fine mesh.

Figure 2 shows the anisotropic damage patterns computed for the different meshes (at the figure top is the cracking pattern experimentally observed (Nooru-Mohamed, 1992)). The left column corresponds to the D_{22} damage field, the right one to the D_{11} damage field, both in nonlocal computations. They exhibit the now classical convergence and mesh independence of the results obtained with a nonlocal model, here in case of anisotropic damage. The application of the shear load up to F_{Max} yields localized damage at the notch tip. The structural failure is then due to the application of the vertical displacement $U(t)$ with mainly mode I cracks represented here in the Continuum Damage Mechanics framework by large D_{22} values. The damage patterns computed corresponds to the crack patterns observed with the rotation of two main cracks represented. The cracks

are not perfectly symmetric with respect to the center of the specimen due to the application of the experimental boundary conditions.

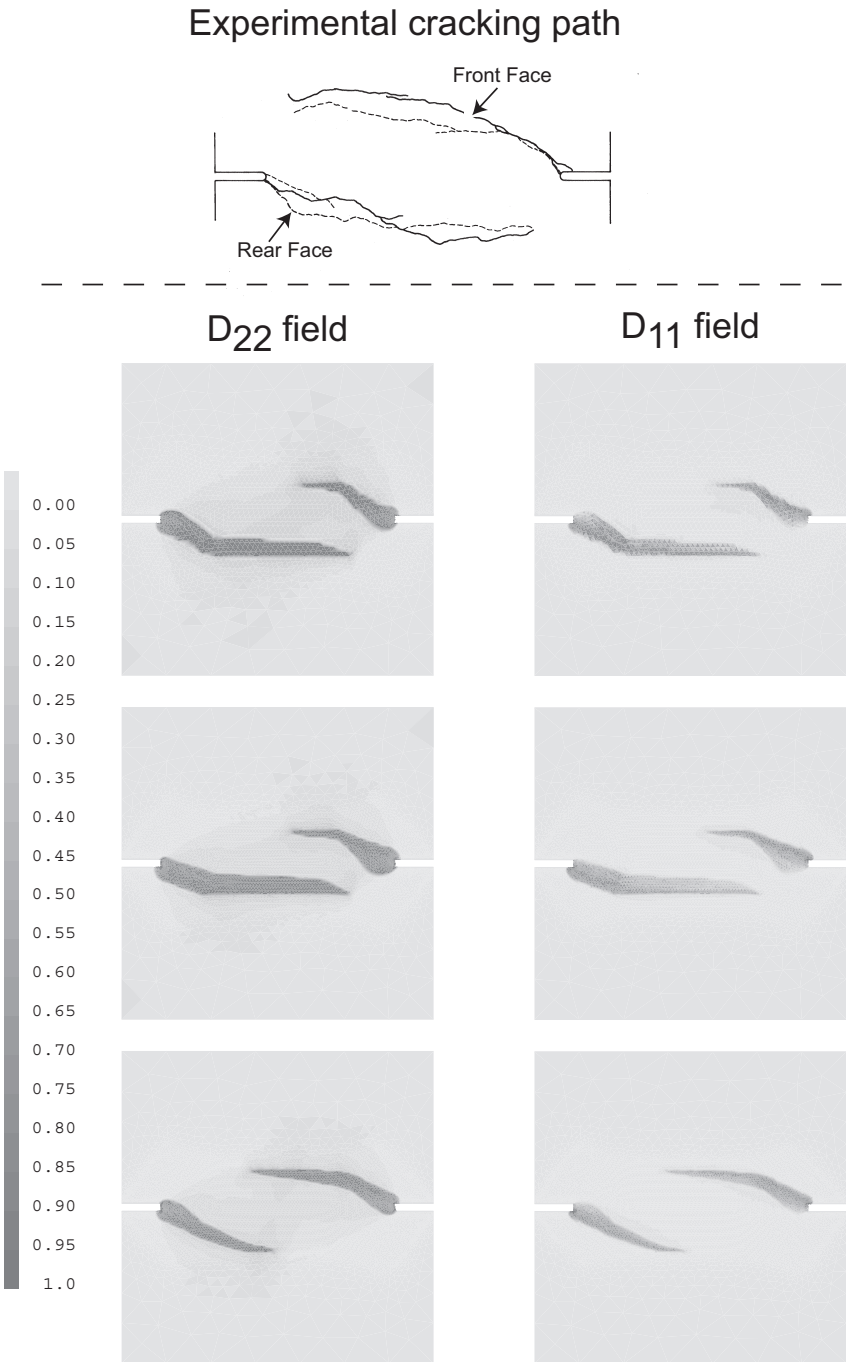

Figure 2: Damage maps for Nooru-Mohamed test at $U = 3.5\ 10^{-3}$ mm– (a) left column: D_{22} fields, (b) right column: D_{11} fields

6.2 *Reinforced concrete structure*

The objectives of this section are to evaluate the robustness and the ability of the anisotropic damage model to deal with a reinforced concrete element

subject to flexion. The structure is a reinforced square cross section beam, subject to three point bend loading. Figure 3 shows geometric features for concrete and steel. During loading, multiple loading paths are encountered in different parts of the beam: tension on the lower part, compression on the upper part, shear near the edge and along the reinforcing bars. The corresponding different features of the constitutive equations are activated at the same time and the occurrence during loading of several competitive cracks usually makes difficult the global convergence scheme. For these reasons, this case-study was part of the international MECA benchmark, launched by E.D.F. to compare and discriminate different 3D constitutive models for concrete (Delaplace and Ghavamian, 2003).

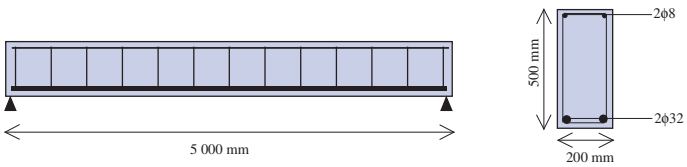

Figure 3: Reinforced concrete beam

For concrete, the material parameters used in the following computations are those of previous section. For steel, elasto-plasticity with linear hardening is considered and the material parameters are imposed by the benchmark: Young's modulus $E = 200000$ MPa, Poisson ratio $\nu = 0.3$, yield stress of 480 MPa, plastic modulus of 20000 MPa. For the computation, a 3D specimen has been meshed with 2 elements in the thickness for a total of 600 eight node parallelepipedic elements. Accounting for the different symmetries of the problem, only one reinforcing steel bar is modelled. The mean dimension of the finite element size is 50 mm.

The monotonic loading is applied up to failure. Two computations with two different characteristic lengths are performed in order to appreciate the effect of the nonlocal length (Gaussian weight function, $\ell_c = 150$ mm and $\ell_c = 250$ mm). The choice $\ell_c = 150$ mm is the more physical as it corresponds here to a characteristic length equal to 3 or 4 times the maximum aggregate size (Bazant and Pijaudier-Cabot, 1989).

As one can see in the D_{11}-damage maps given in Figure 4, due to the reinforcing steel bar implying a flexural rupture the effect of the characteristic length is important on the cracking pattern as it can be seen from damage maps. The choice $\ell_c = 150$ mm is the more appropriate here, as expected. The computation represents quite well the multiple cracks propagation for the characteristic length $\ell_c = 150$ mm.

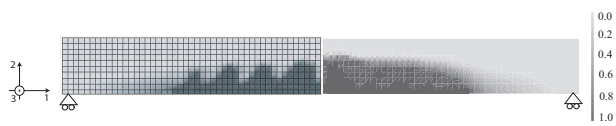

Figure 4: Mesh and D_{11} damage field obtained at the begining of steels yielding (left : $\ell_c = 150$ mm, right: $\ell_c = 250$ mm - left and right correspond to two different computations)

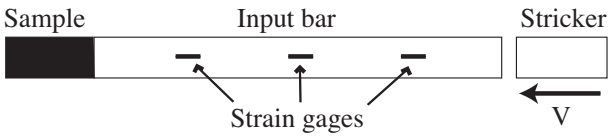

Figure 5: Principle of the dynamic tension test

6.3 *3D dynamics tension test*

In order to get tensile results at very high strain rates, tensile tests by scabbing were developed (Klepaczko and Brara, 2001; Schuler et al., 2006). Figure 5 shows the principle of the test. The setup consists of a striker (launched at the velocity V), an input bar and the tested specimen. The input bar of (Klepaczko and Brara, 2001) experiment has a diameter of 40 mm for a one meter length, while the concrete sample has the same diameter for a length of 120 mm. After the impact of the striker, an incident wave propagates in the input bar. One part of the wave is transmitted into the specimen and another one is reflected at the bar/specimen interface. The transmitted compression wave is reflected at the free end and becomes a tensile wave. This leads to fracture in the spall plane.

Three Finite Element meshes have been used. A coarse mesh is made of 24000 underintegrated 8-nodes brick elements, a medium mesh of 48000 elements and a fine mesh of 96000 elements. At time $t = 0$ the mesh boundaries are free and the experimental pressure wave is applied on the right face of the specimen. The simulation of the test must make it possible to find the rupture of the sample experimentally observed, *i.e.* a single main rupture crack at the distance $X = 65.8$ mm of the impacted face.

Figure 6 shows the damage field D_{11} associated with the axial axe $\vec{e}_1$. When the material is subjected to compression the imposed strain is not sufficient to damage the material. To the opposite, when the state of tension becomes sufficiently large after the compressive wave reflection on the free surface, one obtains a damage D_{11} close to 1 in a cross section. This cross section, which represents the location in which cracking will be initiated, is located at a distance X ranging between 64 and 69 mm from the impacted face. This measure is in good agreement with experimental one.

In order to illustrate the mesh independency (due to the viscous regularization of the delay-damage model), the results are presented on the coarse, medium and fine meshes. The damage maps obtained for the three meshes are shown in Figure 6. One can notice that the width of the localized damage band is the same for the three meshes and equal to approximately $5 \times \ell_c$, therefore of the order of magnitude of a characteristic length introduced from the knowledge of the wave celerity c_L, $\ell_c = c_L \times \tau_c = c_L/D_\infty$. Note that the times steps are different in the three simulations due to the Courant's condition based on the mesh size.

6.4 *Impact on a reinforced concrete slab*

In order to evaluate the ability of the anisotropic damage model to describe the concrete behavior in a case rather complex but representative of an

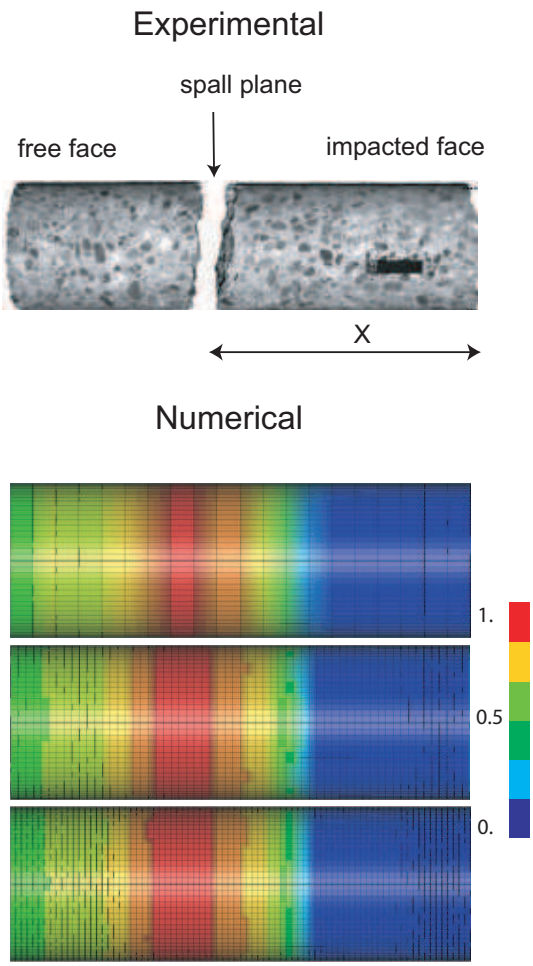

Figure 6: Damage in the concrete sample (D_{11} field, $1 \equiv$ horizontal)

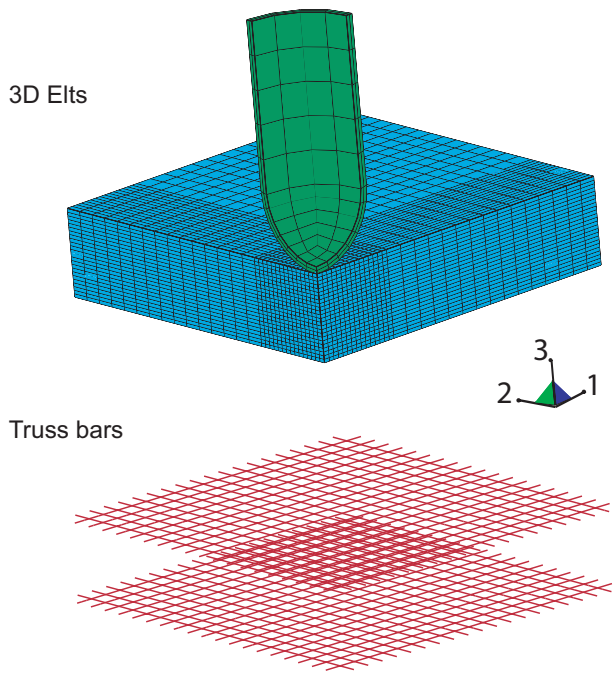

Figure 7: Finite Element mesh

industrial application, a test in which a projectile impacts a concrete slab has been carried out. The projectile is a cylinder representative of a Cessna engine (masse=200 kg, velocity=83,3 m/s, cross section=1 m^2) with an elastic behavior.

Figure 7 shows the finite element mesh used for the simulations on a 4 meters width and 0.5 meters thick slab. The slab is meshed with 24000 3D underintegrated elements and the reinforcements are represented by 2300 truss-bars. The impacted area has a refined mesh whereas the other part of the slab has a coarse one.

Figure 8 shows the damages D_{11}, D_{22} and D_{33} into the slab. One can notice that due to the symmetry condition, the damage D_{11} and D_{22} have a similar pattern. The damage D_{33} represents the cracks in the slab thickness and is representative of the scabbing phenomenon. In our simulation, damages D_{11} and D_{22} are quite large exhibiting a shear rupture of the concrete slab with the apparition of a punch cone as experimentally observed in cases of thin slabs (more precisely of small ratio slab thickness / slab stiffness). In the same time, the damage D_{33} remains small and does not exhibit scabbing.

7 CONCLUSION

A non standard thermodynamics framework for induced anisotropic damage guaranties the positivity of the intrinsic dissipation. A proof is given and the scalar feature $\dot{D} \geq 0$ of a positive damage rate for isotropic modeling is extended to anisotropy as the simple feature $\dot{\boldsymbol{D}} \geq 0$ of a positive damage rate tensor. The convexity of the state potential with respect to the damage variable is not necessary.

An anisotropic damage model is described in the previous non stan-

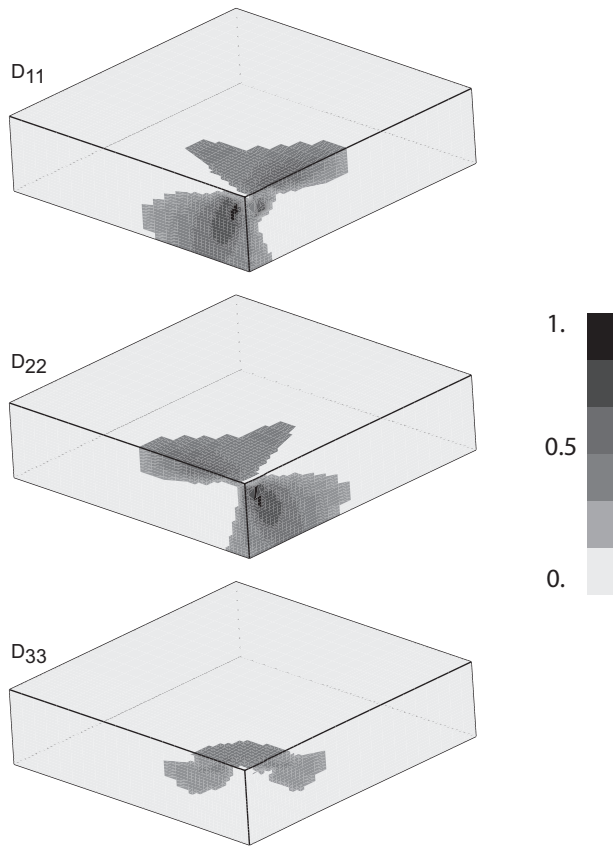

Figure 8: Damage map

dard framework, with a quite low numbers of material parameters (5 including the elasticity parameters for the initial plus an internal length or an internal time for the nonlocal model or plus 2 viscosity parameters for the delay-damage model). The good mathematical properties of the model (differentiability of the state potential, positivity of the dissipation due to anisotropic damage even for complex non proportional loading) prove to be efficient for numerical computations of 3D structures, in both quasi-static and dynamic cases.

References

Aifantis, E. (1987). The physics of plastic deformation. *Int. J. Plasticity*, 3:211–247.

Allix, O. and Deü, J. (1997). Delay-damage modelling for fracture prediction of laminated composites under dynamic loading. *Engineering Transactions*, 45:29–46.

Bazant, Z. P. and Pijaudier-Cabot, G. (1989). Measurement of characteristic length of nonlocal continuum. *Journal of Engineering Mechanics*, 115:755–767.

Billardon, R. and Pétry, C. (2005). Creep damage behaviour of a copper alloy on a large temperature range. In *ASME/ASCE/SES Conference on Mechanics and Materials (McMat2005), 1-3 juin, Baton Rouge, Louisiana, USA*.

Delaplace, A. and Desmorat, R. (2007). Discrete 3d model as complimentary numerical testing for anisotropic damage. *International Journal of Fracture*, 148:115–128.

Delaplace, A. and Ghavamian, S. (2003). *Modèles de fissuration de béton - projet MECA*, volume 7(5). Revue Française de Génie Civil, Lavoisier.

Desmorat, R. (2000). Quasi-unilateral conditions in anisotropic elasticity. *C.R. Acad. Sci. Paris, série IIb*, 328:445–450.

Desmorat, R. (2004). Modèle d'endommagement anisotrope avec forte dissymétrie traction/compression. In *5è journéees du Regroupement Francophone pour la Recherche et la Formation sur le Béton (RF2B), Liège, Belgium, 5-6 july*.

Desmorat, R. and Cantournet, S. (2008). Modeling micro-defects closure effect with isotropic/anisotropic damage. *Int. J. Damage Mechanics*, 17:65–96.

Desmorat, R., Gatuingt, F., Chambart, M., Combescure, D., and Guilbaud, D. (2008). Anisotropic 3d delay-damage model to simulate concrete structures. *Revue Européenne de Mécanique Numérique*, 17:749–760.

Desmorat, R., Gatuingt, F., and Ragueneau, F. (2007). Nonlocal anisotropic damage model and related computational aspects for quasi-brittle materials. *Engineering Fracture Mechanics*, 74:1539–1560.

Dragon, A. and Halm, D. (1996). Modélisation de l'endommagement par mésofissuration : comportement unilatéral et anisotropie induite. *C. R. Acad. Sci., Série IIb*, 322:275–282.

Halphen, B. and Nguyen, Q. (1975). Sur les matériaux standards généralisés. *J. de Mécanique*, 14:39–63.

Klepaczko, J. and Brara, A. (2001). An experimental method for dynamic tensile testing of concrete by spalling. *Int. Journal of Impact Engineering*, 25:387–409.

Krajcinovic, D. (1996). *Damage mechanics*. Elsevier.

Ladevèze, P., Allix, O., Gornet, L., Leveque, D., and Perret, L. (1998). *Computational damage mechanics approach for laminates: identification and comparison with experimental results*, chapter Damage Mechanics in Engineering Materials. Section A. Elsevier, G. Voyiadjis ed.

Ladevèze, P. (1983). On an anisotropic damage theory. In *Proc. CNRS Int. Coll. 351 Villars-de-Lans, Failure criteria of structured media, J. P. Boehler ed. 1993*, pages 355–363.

Ladevèze, P. (1995). Modeling and simulation of the mechanical behavior of cmcs. *High Temperature Ceramic-Matrix Composite, A. G. Evans and R. Naslain eds, Ceramic Transaction*, 57:53–64.

Leckie, F. and Onat, E. (1981). *Tensorial nature of damage measuring internal variables*, chapter Physical Non-Linearities in Structural Analysis, pages 140–155. J. Hult and J. Lemaitre eds, Springer Berlin.

Lemaitre, J. and Desmorat, R. (2005). *Engineering Damage Mechanics : Ductile, Creep, Fatigue and Brittle Failures*. Springer.

Lemaitre, J., Desmorat, R., and Sauzay, M. (2000). Anisotropic damage law of evolution. *Eur. J. Mech., A/ Solids*, 19:187–208.

Mazars, J. (1984). *Application de la mécanique de l'endommagement au comportement non linéaire et à la rupture du béton de structure*. PhD thesis, Thèse d'Etat Université Paris 6.

Mazars, J., Berthaud, Y., and Ramtani, S. (1990). The unilateral behavior of damage concrete. *Eng. Fract. Mech.*, 35:629–635.

Nooru-Mohamed, M. (1992). *Mixed-mode fracture of concrete: An experimental approach*. PhD thesis, Delft University of Technology, The Netherlands.

Papa, E. and Taliercio, A. (1996). Anisotropic damage model for the multiaxial static and fatigue behaviour of plain concrete. *Engineering Fracture Mechanics*, 55:163–179.

Peerlings, R., de Borst, R., Brekelmans, W., and de Vree, J. (1996). Gradient-enhanced damage model for quasi-brittle materials. *Int. J. Num. Meth. Engng*, 39:391–403.

Pijaudier-Cabot, G. and Bazant, Z. (1987). Nonlocal damage theory. *J. Engng Mech., ASCE*, 113:1512–1533.

Pijaudier-Cabot, G., Haidar, K., and Dubé, J.-F. (2004). Non-local damage model with evolving internal length. *International journal for numerical and analytical methods in geomechanics*, 28:633–652.

Ragueneau, F., Delaplace, A., and Davenne, L. (2003). Mechanical behavior related to continuum damage mechanics for concrete. *Revue Française de Génie Civil*, 7:635–645.

Schuler, H., Mayrhofer, C., and Thoma, K. (2006). Spall experiments for the measurement of the tensile strength and fracture energy of concrete at high strain rates. *International Journal of Impact Engineering*, 32:1635–1650.